Polymer Degrad Stab: doi.org/10.1016/j.polymdegradstab.2020.109220

Novel Metal Complexes as Potential Synergists with Phosphorus Based Flame Retardants in Polyamide 6.6

Alistair F. Holdsworth[1a], A. Richard Horrocks[1b] and Baljinder K. Kandola[1]

Affiliations: 1) - IMRI, University of Bolton, Deane Road, Bolton, UK, a) Now at School of Chemistry, University of Manchester, Oxford Road, Manchester, UK b) Corresponding Author: a.r.horrocks@bolton.ac.uk

Abstract

Aluminium (AlW), tin (II) (SnW) and zinc (ZnW) tungstates were previously found to increase char formation in polyamide 6.6 (PA66), but have never before been studied for their potential as synergists when present with phosphorus-containing (PFRs) flame retardants. We investigate this gap in the scientific knowledge in this publication. Tungstate-PFR interactions of PA66 composites were investigated by thermal analysis, limiting oxygen index (LOI), UL94, cone calorimetry and evolved gas analysis (TGA-FTIR).

Of the three tungstates, AlW in the presence of aluminium diethylphosphinate (AlPi) or a mixture of AlPi and melamine polyphosphate (MPP), promotes the highest level of flame retardancy in terms of a balance of high LOI, V-rating and TGA residual char in air at 500°C and reduction in cone calorimetric peak heat release rate (R_{PHRR} = 80%). This observation has been related to AlW having the highest Lewis acidic properties. While zinc tungstate displays the lowest levels of interaction with either PFR, it shows significant smoke suppressant properties.

Elemental analysis of cone calorimetric chars suggests that while some loss of phosphorus occurred from SnW/AlPi/MPP-containing composites, most likely via volatile diethyl phosphinic acid formation, nearly 10% reduction also occurred in the Sn/W molar ratio indicating some volatilisation of tin. The TGA (in air)-FTIR results for carbon dioxide, ammonia and hydrocarbon fuel species evolution enabled discussions of the effect that each tungstate had on the flame retardant mechanisms operating.

Keywords: Polyamide 6.6, tungstates, synergism, phosphorus, aluminium diethylphosphinate, melamine polyphosphate, flammability, thermal analysis, cone calorimetry, FTIR

Polymer Degrad Stab: doi.org/10.1016/j.polymdegradstab.2020.109220

1.0 Introduction

In recent years, the currently available commercial flame retardants (FRs) have come under increasing scrutiny with regard to their toxicology and environmental sustainabity [1]. With the development of new compounds, however, must come an understanding of their function, if any, and whether or not they have commercial potential, especially when the use of synergists and co-species to increase FR performance may enable reduced total fire retardant loadings [2], maintaining mechanical properties in high-value polymers.

Of particular note are the concerns raised over the environmental toxicity of several brominated flame retardants (BrFRs) and their common synergist, antimony trioxide (ATO) [1, 3-5], which also has questionable toxic, and potentially carcinogenic properties, although some phosphorus-containing flame retardants (PFRs) have also been questioned [1, 2, 3]. Commercially viable alternatives to ATO such as zinc stannate (ZnS), are well-known and have had their mechanisms studied in some depth [6-8]. These stannates also offer the additional property of smoke reduction [6] when present as synergists with BrFRs and there has been some more recent evidence of positive interactions with phosphorus-containing flame retardants (PFRs) [9]. Not surprisingly, the replacement of both BrFRs and ATO has focussed attention on benign inorganic alternatives such as magnesium and aluminium hydroxides [10], which, though relatively cheap, require very high levels (>50 wt%) present in the polymer in order to generate effective flame retardancy. Similarly, it is well established that metal oxides such as ZnO, Fe_2O_3 and SnO can provide an inherent degree of flame retardancy in some polymers. Most of these inorganic species have little effect on the degradation pathway of a polymer, although Kicko-Walczak [7] has proposed that SnO, formed from the degradation of zinc stannate in the presence of a BrFR may interact with hydrogen radicals generated in the flame in the vapour phase. Whether a similar mechanism operates with PFRs, especially these known to function in the vapour phase, is not known.

A recent study by ourselves screened six metal (calcium, manganese (II), iron (II), copper (II), tin (II) and zinc) oxalates for their potential flame retardant and/or synergistic activity in polyamide 6.6 (PA66) in the absence and presence of selected flame retardants [11, 12]. Results suggested that only zinc oxalate (ZnOx) offers both possible flame retardant activity in terms of enhanced thermogravimetric analytical (TGA) residue formation ≥ 500 ^{o}C, coupled with acceptable stability in molten PA66. Furthermore, when compounded with

PA66 in the presence and absence of either aluminium diethyl phosphinate (AlPi)-based or selected polymeric bromine-containing flame retardants, limiting oxygen index (LOI) values increased in most PA66/ZnOx/FR blends. UL94 test V-ratings were disappointingly low, however, and more likely than not, "fails".

Subsequently, we established a high throughput protocol [12, 13] method for the rapid synthesis, screening and initial fire testing of 151 inorganic compounds potentially suitable as inorganic additives for use in a typical engineering polymer such as polyamide 6.6 (PA66). Of these, a number of metal tungstates, which have received little to no attention to date, were identified as potential flame retardants in PA66 using using LOI, UL94 and cone calorimetry methods. Three examples in particular proved of interest: aluminium, tin (II) and zinc; $Al_2(WO_4)_3$, $SnWO_4$ and $ZnWO_4$ respectively, hereafter referred to as AlW, SnW and ZnW, each of which when present at 5 wt% in PA66 showed reductions in both peak and total heat release rates relative to the pure polymer and yielded the most easily processible plaques. Among these, AlW demonstrated the highest flame retardancy with LOI value of 23 vol%. However, while their use alone is insufficient to promote the high levels of flame retardancy, their possible interaction or even synergism with other flame retardants, such as noted previously with zinc oxalate [11], could demonstrate their suitability in augmenting the effectiveness of the latter primary FRs.

In this publication, we investigate for the first time the potential interactions and possible synergisms between these three compounds and two phosphorus-containing flame retardants, which have been shown to have high effectiveness in polyamides, namely aluminium diethylphosphinate (AlPi)) and a mixture of this compound with melamine polyphosphate (AlPi/MPP) [9, 14, 15]. Using TGA, TGA-FTIR and cone calorimetry in particular, the degree of possible interactions and underlying mechanisms are reported.

2.0 Experimental

2.1 Materials

The three tungstates (AlW, SnW and ZnW) were synthesised and characterised as previously reported [12]. These materials were calcined at 240 ^{o}C (under vacuum for SnW, to suppress oxidation). 100% PA66 was

acquired from Invista Engineering Polymers (compounding grade, 100% PA66, m.pt. 260 ^{o}C, MFI 19.56 g/min @ 280 ^{o}C), UK; AlPi and AlPi/MPP were obtained as the commercial formulations Exolit 1230 and Exolit 1311 respectively, supplied by Clariant Ltd, Switzerland. Melamine polyphosphate was supplied by as Melapur 200 (Ciba) and used without further purification.

2.2 Polymer Composite Compounding

Compounding of all PA66 formulations was undertaken using a laboratory-scale Thermo-Scientific twin-screw extruder. The six barrel heating elements were set progressively at 250, 255, 260, 265, 270 and 275 ^{o}C respectively and a screw speed of 350 rpm was used. Prior to compounding, all PA66 polymer pellets and previously calcined flame retardant additive powders were dried at 80 ^{o}C for at least 36 h before processing. Compounded formulations are listed variously below in Section 3 unless otherwise stated. Dry compounded pellets were pressed into plaques (170 x 170 x 3 mm) using a hot press at 260 ^{o}C with a pressure of 20 kg/cm^2, followed by cutting into strips 12.7 mm wide for UL94 and LOI testing and 75 x 75 mm plaques for cone calorimetric analysis, where appropriate.

2.3 Fire Testing

Compounded PA66 samples were assessed for Limiting Oxygen Index (LOI) according to ASTM 2863 and subjected to the UL-94 test in the vertical orientation, according to ISO 1210. UL-94 tests were performed in triplicate due to the volume of samples under assessment and the limited supply of each experimental formulation, as this work was conducted as part of a much larger study. Cone calorimetry was also performed on those samples which produced viable plaques using a 50 kW/m^2 heat flux (FTT cone calorimeter, Fire Testing Technology, UK) according to ISO 5660. Several parameters were determined, namely the times-to-ignition, T_{ig}, time-to-flame-out, T_{fo}, time-to-peak heat release rate, T_{PHRR}, the peak heat release rate, PHHR, total heat release rate, THR and total smoke release, TSR.

2.4 Thermogravimetric and TGA-FTIR Analysis

Simultaneous thermogravimetric and differential thermal analyses (TGA/DTA) were conducted using a TA Instruments SDT 2960 analyser, with nominal sample masses of 10-12 mg. Experiments were undertaken under a 100 ml/min flow of either air or nitrogen from ambient to 600 ^{o}C at a heating rate of either 10 or 20 ^{o}C/min, the latter being used for the TGA-FTIR evolved gas analysis experiments. For these, the exhaust from the SDT 2960 thermal analytical module was connected to a heated gas cell (Thermo-Fisher Nicolet iS10) maintained at 250 ^{o}C mounted on a Thermo-Fisher Nicolet iS7 FTIR spectrometer via a heated, stainless steel gas line at 250 ^{o}C. An isothermal starting stage was incorporated before the ramping stage whereby the system was equilibrated at 100 ^{o}C for 5 minutes, allowing for thorough drying of the sample, equilibration of the atmosphere in the TGA/DTA furnace and for the FTIR background effluent to be collected. FTIR data acquisition was started when the TGA/DTA ramp began. There was a delay between recorded TGA/DTA data and FTIR data of approximately 45 seconds due to the gas transit time from the exhaust of the TGA to the FTIR cell.

Several key evolved species, namely carbon dioxide, ammonia and aliphatic species including cyclopentanone and its derivatives that are possible fuels (designated CH_x), were identified as being key indicators of significant mechanistic stages in the degradation of polyamide 6.6 (see below). IR absorption peaks monitored were CO_2 at 2357 cm^{-1}, NH_3 at 968 cm^{-1} and aliphatic CH_x at 2933 cm^{-1} (which would include cyclopentanone and other hydrocarbon fuel species) and respective absorptions were recorded over time and adjusted to account for TGA/DTA sample size by dividing each data point by the starting TGA/DTA sample mass after equilibration at 100 ^{o}C. Additionally, the carbon dioxide profiles acquired under nitrogen and all profiles under air were corrected for atmospheric interference by the addition or subtraction of the lowest value of each spectral trace to give a zero baseline. The amounts of CH_x, NH_3 and CO_2 produced were calculated by summing all the FTIR intensity data points in arbitrary units.

2.5 Char analysis

Selected chars from cone calorimetric studies were analysed by a Thermo-Scientific Nicolet iS10 FTIR analyser using a diamond lens attenuated total reflection (ATR) adapter for the analyser. Detection of key metals within selected compounded chips samples and derived chars was undertaken by X-ray Fluorescence (XRF)

experiments using the facilities of William Blythe Ltd., comprising a PANalytical Axios analyser and the Omnic software suite.

2.6 Synergistic Effectivity

The synergistic effectivities [16] were calculated using Equation 1, where Es is the synergistic effectivity, and X_p, X_s, X_{fr} and $X_{[fr+s]}$ are the measured flammability parameters LOI and the percentage reduction in cone calorimetrically determined peak heat release rate, R_{PHRR}, see below) for pure PA66, PA66 containing the synergist, PA66 containing the primary flame retardant and PA66 containing both respectively.

$$Es = [X_{[fr+s]} - X_p] / [(X_{fr} - X_p) + (X_s - X_p)] \quad \text{(Eq 1)}$$

3.0 Results and Discussion

3.1 Thermal stability and flammability Studies

3.1.1 Effect of added flame retardants AlPi and AlPi/MPP alone on PA66 flammablity

Prior to being able to develop an experimental matrix that would enable any favourable interactions occurring between AlW, SnW and ZnW and the two selected phosphorus-containing flame retardants (PFRs), AlPi and AlPi/MPP to be identified, a scoping study was undertaken to determine the critical levels of AlPi and AlPi/MPP. Typical commercial levels of AlPi and AlPi/MPP recommended to achieve UL94 test V-O ratings in PA66 are in the range 15-18 wt% [14]. In order to identify the effect of PFR concentration on PA66 flammability, both compounds were separately incorporated into PA66 at 7.5, 10, 12.5 and 15 wt% and then subjected to thermogravimetric analysis in air and nitrogen, and LOI, UL94 and cone calorimetric testing to determine their thermal and flammability behaviour (see Table 1).

The TGA plots in air for the PA66 control, the PA66/AlPi(7.5 wt%) and the PA66/AlPi/MPP(10 wt%) compounded samples are presented in Figures 1(a) and (b) respectively. It has been reported elsewhere that

char residue from PA66 alone heated above 450 °C under air is greater than when under nitrogen [8, 17] demonstrating that oxygen increases char formation, and so with respect to the potential flame resisting properties of the AlPi and AlPi/MPP combinations, further slight increases are noted.

Table 1 lists the TGA onset temperatures of volatilisation at 5% mass loss, $T_{5\%}$, in air of each formulation in order to assess the effects of each PFR on the initial stages of PA66 thermal degradation. For the PA66/AlPi sample set relative to the pure PA66 curve, the presence of 7.5 wt% AlPi reduces $T_{5\%}$ from 386 °C for pure PA66 to 368 °C with little further change with increase in AlPi concentration. For the PA66/AlPi/MPP samples, $T_{5\%}$ values in air continue to reduce with higher flame retardant concentration.

Table 1: TGA (in air), UL94, LOI and cone calorimetric results for PA66/AlPi and PA66/AlPi/MPP samples

Sample and FR concentrations, %	$T_{5\%}$, °C	UL94			LOI	Cone calorimetric data				
		1	2	3	vol%	$T_{ig.}$ s	T_{fo}, s	T_{burn}, s	THR, MJ/m^2	PHHR, kW/m^2
PA66	386	V-2	Fail	Fail	22.5	55	146	91	115	1709
AlPi-7.5	368	Fail	Fail	Fail	28.2	40	143	103	115	1025
AlPi-10.0	374	V-0	V-0	V-0	31.5	43	159	116	115	906
AlPi-12.5	377	V-0	V-0	V-0	33.3	37	136	99	100	841
AlPi-15.0	374	V-0	V-0	V-0	33.9	39	134	95	90	831
AlPi/MPP-7.5	365	V-2	V-2	Fail	26.4	50	182	132	110	724
AlPi/MPP-10.0	338	V-0	V-1	Fail	28.2	55	181	126	130	666
AlPi/MPP-12.5	337	V-0	V-0	V-0	28.5	58	183	125	135	627
AlPi/MPP-15.0	331	V-0	V-0	V-0	28.5	67	197	130	140	531

Key: 1, 2 and 3 are the UL94 replicates to show reproducibility, T_{ig}, T_{fo} and T_{burn} are the times to ignition, flame out, total burn ($T_{fo} - T_{ig}$) and THR and PHRR are the total and peak heat release rates respectively

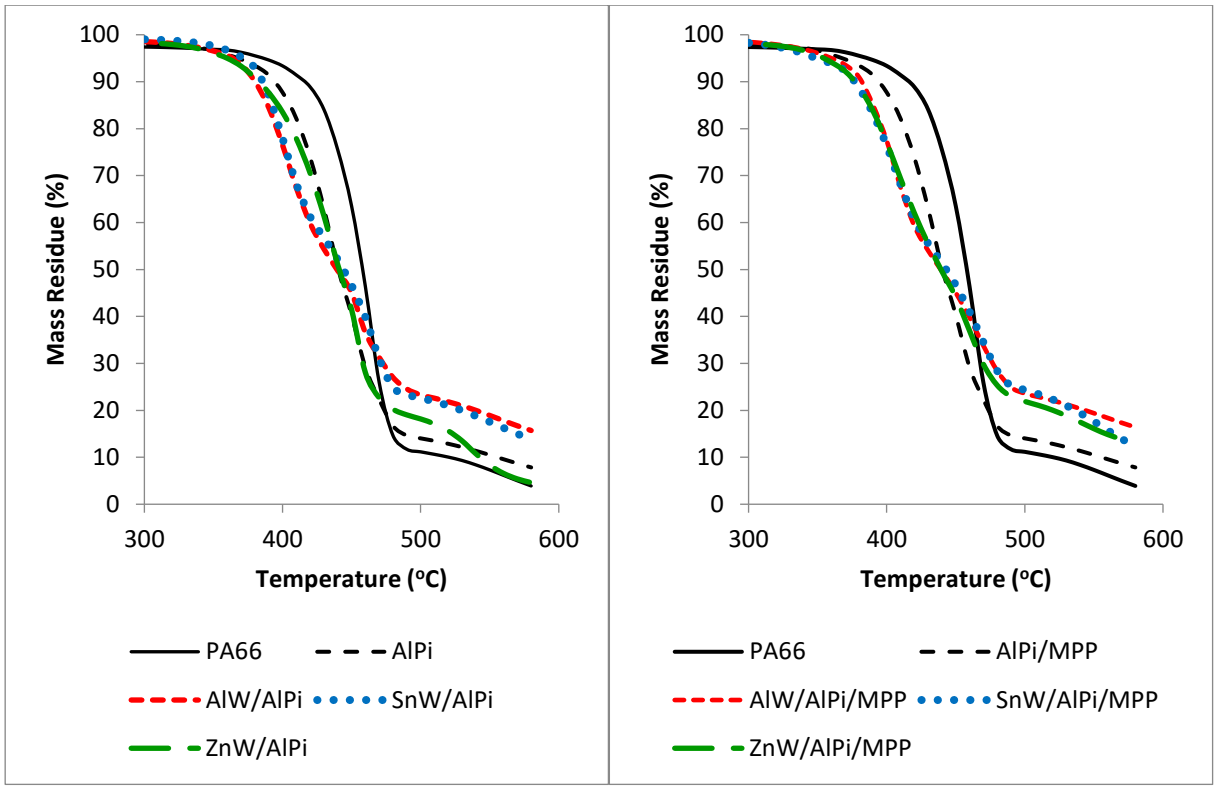

Figure 1: TGA response curves in air at 10 deg/min, of (a) PA66 and PA66/AlPi (7.5 wt%) and (b) PA66 and PA66/AlPi/MPP (10 wt%) in the absence and presence at 5 wt% of the tungstates AlW, SnW or ZnW.

Table 1 lists the recorded flammability testing parameters for all samples containing flame retardant alone from which it is evident that consistent V-0 ratings are obtained in PA66/AlPi composites at 10 wt% levels whereas in the PA66/AlPi/MPP samples, 12.5 wt% additive levels are required. It is interesting to note that both 7.5 wt% AlPi and 10 wt% AlPi/MPP formulations yielded LOI = 28.2 vol%. However, AlPi-only containing samples finally achieved an LOI value of 33.9 vol%, considerably higher than that for AlPi/MPP samples (28.5 vol%) at the same total 15 wt% concentration. Of the cone calorimetric parameters recorded, only the peak heat release values, PHRR, show really significant changes as the concentration of each flame retardant is increased with formulations containing both AlPi and MPP showing greater reductions than those containing AlPi alone at similar concentrations. Times to flameout for AlPi/MPP samples, however, increase significantly with increasing concentration, presumably because of the char-promoting effect of melamine polyphosphate, which is also most likely the cause of the greater PHRR reductions [17]. This is also reflected in the increased

total heat release,THR, values whereas the largely vapour phase active AlPi alone, causes a reduction in THR at the highest concentrations.

3.2 Effect of added tungstates

Based on the results in Table 1, samples selected for compounding with each tungstate at 5 wt% were 7.5 wt% of AlPi alone and 10 wt% for the combined AlPi/MPP PFRs (see Table 2) both of which failed to achieve V-0 ratings. Thus it was anticipated that any additional effect of added tungstate would be more easily observed as an elevation in V-rating. The tungstate level of 5 wt% was chosen because typically synergists such as ATO and the zinc stannates are rarely used above this level [6, 8], and difficulties compounding inorganic additives such as AlW at higher concentrations, including 7.5 wt% in PA66 were previously encountered [12, 13].

Of the pressed PA66 sheets for formulations containing each of three tungstates with either 7.5 wt% AlPi or 10 wt% Al/Pi/MPP, only the PA66/ZnW/AlPi formulation showed any evidence of voids. TGA/DTA responses were recorded for each formulation under air (see Figures 1(a) and (b) for TGA responses) at 10 ^{o}C/min and the respective sample $T_{5\%}$, the DTG maximum temperatures, T_{max}, and residues at 500 and 580 ^{o}C are recorded in Table 2. Residues at 500 ^{o}C (R_{500}) are considered to represent residues with maximum carbonaceous char content and 580 ^{o}C (R_{580}) values, those where significant carbon oxidation has occurred under the flowing air atmosphere. Although this latter temperature appears to have been chosen in a rather arbitrary manner (see Figures 1(a) and (b)), while PA66 alone still shows R_{580} = 3.9%, the ZnW/AlPi formulation has R_{580} = 4.6%, a value close to the initial 5% ZnW present. To allow for the addition of 5 wt% tungstate, assuming their presence still at 500^{o}C, values in brackets equal (R_{500} – 5) wt%, thereby representing the carbon and residual AlPi or AlPi/MPP contents.

Figure 1(a) shows that relative to the PA66/AlPi response, although all three tungstates have minimal effect on the $T_{5\%}$ value but increase residues at 500 ^{o}C. However, correcting for 5 wt% tungstate content, the bracketed values in Table 2 show that presence of AlW and SnW has increased char contents when AlPi alone is present but has reduced chars when AlPi/MPP is present suggesting some form of negative tungstate-MPP reaction. A similar inference may be drawn when ZnW and AlPi are together in the composite. While the TGA

responses for the PA66/AlW/AlPi and PA66/SnW/AlPi formulations are almost identical and exhibit a slight shoulder at about 450 °C, the addition of zinc tungstate has had little influence on the main volatilisation stage compared to the PA66/AlPi formulation and lacks this shoulder. Figure 1(b) shows similar behaviour for the PA66/AlPi/MPP/tungstate formulations relative to the tungstate-free sample and their TGA responses in air are all very similar with again, a slight shoulder appearing in the 450 °C region.

Table 2: TGA/DTA results of the PA66 samples containing 7.5 wt% AlPi or 10 wt% AlPi/MPP

Sample	Composition, %			TGA/DTG (Air)			
	PA66	MW*	PFR	$T_{5\%}$, °C	T_{max}, °C	R_{500}, wt%**	R_{580}, wt%
PA66	100	-	-	386	461	11.2	3.9
AlPi	92.5	-	7.5	368	437	14.0	7.8
AlPi/MPP	90	-	10	368	433	21.5	11.5
AlW/AlPi	87.5	5	7.5	364	405	23.3(18.3)	15.7
AlW/AlPi/MPP	85	5	10	360	407	23.6(18.6)	16.4
SnW/AlPi	87.5	5	7.5	372	401	22.6(17.6)	13.8
SnW/AlPi/MPP	85	5	10	349	408	24.4(19.4)	12.4
ZnW/AlPi	87.5	5	7.5	360	455	18.2(13.2)	4.6
ZnW/AlPi/MPP	85	5	10	355	407	21.9(16.9)	13.2

Key: $T_{5\%}$ is the temperature to 5% mass loss, T_{max} is the DTG peak temperature and R_{500} and R_{580} are the residues levels at those temperatures respectively (in °C); * MW signifies each metal tungstate, **bracketed values = (R_{500} -5)%

DTG T_{max} values under air are for PA66/AlPi samples in the presence of AlW and SnW are further reduced but in the presence of ZnW, increased from 437 to 455 °C. This suggests that there is an interaction between ZnW and AlPi during thermal degradation of PA66 such that the DTG maximum now coincides with the temperature of the slight shoulder exhibited by the other tungstate/AlPi formulations (see also Figure 1(a)). Interestingly, this formulation shows the lowest additional char R_{500} value and no significant increase in char at 580 °C.

Increases in R_{580} values in air relative to pure PA66 when either AlPi or AlPi/MPP are added is a consequence of increased char formation and formation of aluminium phosphate, especially in the latter [13, 14] and addition of either AlW or ZnW promotes further increases apart from the ZnW/AlPi/MPP formulation which shows a significant reduction suggesting volatilisation of the flame retardant components has occurred.

Table 3 lists the values of UL94 rating and LOI for each sample and respective controls, including those

previously published for PA66/tungstate composites [12]. It is evident that the addition of each tungstate to the PA66/AlPi formulation has little if any additional effect on the LOI value, although UL94 ratings show a slight tendency to achieve V-2 when tin and zinc tungstates are present as opposed to a "fail" when absent (see also Table 1). With respect to the PA66/AlPi/MPP formulation, addition of aluminium and zinc tungstates actually reduces the LOI value significantly with parallel reductions in UL94 performance.

The heat release rate curves of all compounded samples are presented in Figures 2(a) and (b) and flame-out times, T_{fo},THR, PHRR and total smoke, TSR, values are listed in Table 3. It is evident that while the presence of either 7.5 wt% AlPi or 10 wt% AlPi/MPP reduces the PHRR values considerably with respect to the PA66 control, further reductions are observed when each of the three tungstates are present. In particular, those containing MPP showing the lowest values , in particular AlW/AlPi/MPP and SnW/AlPi/MPP formulations with the lowest PHRR values of 342 and 300 kW/m^2 recorded, representing 80 and 82% reductions respectively compared to pure PA66. These results, unlike the respective THR results (see below), do not reflect the relative TGA-determined char-forming characteristics in Table 2, although the apparent volatility of the ZnW/AlPi/MPP composite could relate to its having the highest reduction in R_{PHRR} value of 82.4% relative to pure PA66, which appears to be in contrast to its relatively low LOI of 24.9 vol%.

Reductions in flameout times are noticeable in the PA66/tungstate /AlPi formulations in the order ZnW > SnW > AlW and the converse appears to be the case when MPP is present, with increases in the order AlW > SnW > ZnW with respect to the PA66/AlPi/MPP sample. These effects can perhaps be attributed to the formation of more cohesive barriers by the PA66/tungstate/AlPi/MPP composites than PA66/AlPi/MPP alone because of metal complex formation within the residues [17], although relative differences in R_{580} values, that reflect inorganic residual contents in the main, do not reflect this proposal.

Total heat release (THR) values for tungstate-flame retardant combinations show fluctuating values with respect to the control PA66 value, although apart from AlW/AlPi/MPP and SnW/AlPi/MPP formulations, which show higher values, general decreases are observed for tungstate/AlPi combinations. The presence of MPP, may be generally associated with increased char at 500^{o}C (see Table 2), which on combustion will lead to increased total heat release, assuming that the additional char is fully burnt.

Total smoke release, TSR, values show that addition of either PFR more than doubles the smoke generated while the presence of each tungstate alone has a relatively small effect as previously reported [12]. Addition of both AlPi and tungstate produces little or no change in smoke generation with respect to the respective AlPi-only containing formulations apart from that containing ZnW which has a marked smoke suppressing effect. While the further addition of MPP has a marginally smoke-increasing effect, the suppressing effect of ZnW is still apparent.

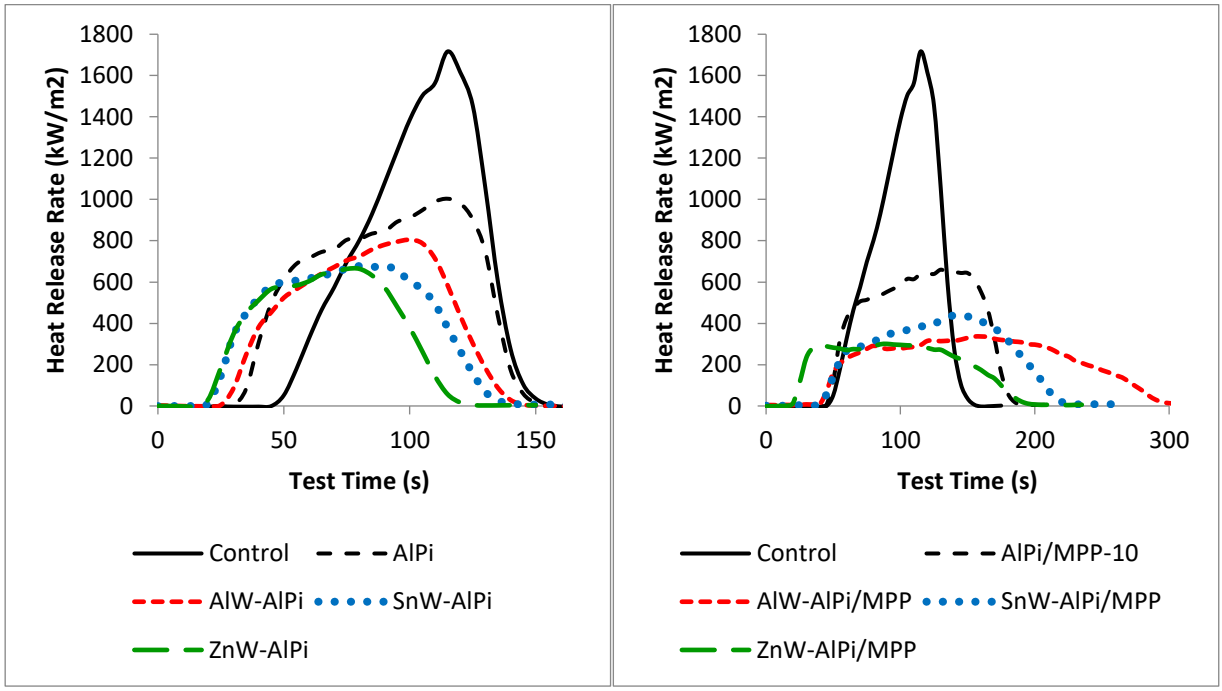

Figure 2: Cone calorimetry heat release rates of (a) PA66/AlPi (7.5 wt%) and (b) PA66/AlPi/MPP (10 wt%) formulations in the presence and absence of 5 wt% of each of the three tungstates, AlW, SnW and ZnW; the PA66 control response is present in each figure.

Polymer Degrad Stab: doi.org/10.1016/j.polymdegradstab.2020.109220

Table 3: Formulations, principal flammability parameters and derived synergistic effectivities for tungstate-phosphorus-containing formulations

Sample	Composition, wt%											
	PA66	Tungstate	PFR	UL-94**	LOI, vol%	$E_{s(LOI)}$	T_{fo}, s	THR, MJ/m^2	PHRR, kW/m^2	TSR, m^2/m^2	R_{PHRR}, %***	$E_{s(PHRR)}$
PA66	100	-	-	F/V-2	22.5	-	144	115	1709	723	-`	-
AlPi	92.5	-	7.5	F	28.2	-	143	115	1025	1736	32.4	-
AlPi/MPP	90	-	10	V-0/V-1/F	28.2	-	181	130	666	1660	44.2	-
AlW*	95	5	-	V-0/V-2/F	23.0	-	146	110	1156	927	30.4	-
SnW*	95	5	-	F/V-2	22.0	-	134	85	954	939	40.0	-
ZnW*	95	5	-	F	21.5	-	138	110	1190	638	57.6	-
AlW/AlPi	87.5	5	7.5	V-0	28.1	0.90	143	100	815	1580	52.3	0.72
AlW/AlPi/MPP	85	5	10	F	25.6	0.54	310	160	342	1814	80.0	0.87
SnW/AlPi	87.5	5	7.5	F/F/V-2	28.4	1.04	134	80	863	1731	49.5	0.55
SnW/AlPi/MPP	85	5	10	V-0/V-1/F	28.8	1.11	229	140	442	1860	74.1	0.73
ZnW/AlPi	87.5	5	7.5	F/F/V-2	27.2	0.83	118	80	683	1163	60.0	0.85
ZnW/AlPi/MPP	85	5	10	V-2/V-2/F	24.9	0.42	201	90	300	1246	82.4	0.94

Notes: * Values from Ref. 12; ** A single rating indicates that all 3 test results achieved that value, otherwise individual test values given; F=fail, ***R_{PHRR}, % is the percentage reduction in PHRR with respect to PA66

Synergistic effectivity values calculated based on LOI and the percent reduction in PHRR (R_{PHRR}) values are also listed with respect to the interactions between the added tungstate and the respective AlPi or AlPi/MPP flame retardant formulation present and reflect these changes in both parameters. Note that in calculating the $E_{s(LOI)}$ values, the factor $(LOI_s - LOI_p)$ (see equation (1) above) is equated to zero. This is because as seen in the Table 3, the inserted data for the LOI values of each tungstate alone in PA66 taken from reference 12, indicates that apparent reductions for SnW and ZnW exist with respect to the pure PA66 ascribed to the modification of melt dripping by their presence. Thus, it assumed that the effect on each tungstate on the LOI is effectively zero in terms of their exerting a real flame retarding effect.

However, the fire models for LOI and PHRR determination are very different with the former representing a threshold ignition parameter and the latter a reaction-to-fire parameter. It is therefore possible to consider each set of Es values with respect to these different characteristics. That the $E_{s(LOI)}$ values for each tungstate in combination with each PFR range from 0.42-1.11 suggests that each is adding to overall flame retardant behaviour in an additive manner for AlW and ZnW and a slightly synergistic manner for SnW. The small difference in $E_{s(LOI)}$ values between the SnW/AlPi (1.04) and SnW/AlPi/MPP (1.11) formulations suggest a marginal improved effect as a consequence of MPP presence. This difference is not reflected in the AlW and ZnW respective formulations where the presence of MPP has the reverse effect. When comparing $E_{s(LOI)}$ values with UL94 results, however, no simple correlation exists although formulations achieving V-0 ratings (either as a whole or in part) have $E_{s(LOI)} > 0.9$.

Inspection of the $E_{s(PHRR)}$ values shows that the presence of a tungstate offers some level of additional flame retarding effect during the post-ignition stage with ZnW-containing formulations generally giving higher values of 0.85 or greater. Comparison with additional TGA char values in Table 2 does not suggest that this effect is directly linked to additional char ($(R_{500}-5)\%$) formation at 500°C.

3.1.3 Role of melamine polyphosphate (MPP)

Because the presence of MPP is reported to confer condensed phase activity when present with AlPi in PA66 [15], the effects of adding AlW, SnW and ZnW at 5 wt% levels together with melamine polyphosphate alone (at 10 wt%) were investigated. The sample compositions and analyses of TGA responses in air are presented in Table 4 together with R_{500} values corrected for the presence of 5wt% tungstate.

Table 4: PA66/MPP sample compositions and TGA data in air and nitrogen

Sample	Composition, wt%			TGA/DTG (Air)			
	PA66	MPP	Tungstate	$T_{5\%}$, °C	T_{max}, °C	R_{500}, wt%*	R_{580}, wt%
PA66	100	-	-	386	461	11.2	3.9
MPP	90	10	-	352	380	15.4	10.5
AlW/MPP	85	10	5	351	381	17.2(12.2)	11.5
SnW/MPP	85	10	5	351	387	20.2(15.2)	12.7
ZnW/MPP	85	10	5	354	381	19.4(14.4)	11.8

Key: $T_{5\%}$ is the temperature to 5% mass loss, T_{max} is the DTG peak temperature and R_{500} and R_{580} are the residues levels at those temperatures respectively (in °C). * bracketed values = (R_{500} -5)%

The addition of MPP alone reduces the $T_{5\%}$ values but addition of additional tungstate has little further effect as noted also in Table 2 when AlPi is present. A similar effect is observed for T_{max} values. As seen for the corrected TGA residues T_{500}, addition of each tungstate does not increase char but in some cases, notably AlW, decreases it. Again, T_{580} values following addition of tungstate show only marginal increases suggesting that volatilisation of the inorganic components has occurred, an effect also noted in Table 2 when AlPi was also present. However, the very low T_{580} value observed for the ZnW/AlPi/MPP sample is not reflected in that for the ZnW/MPP composite showing that there is a complex volatilisation interaction occurring in the former.

The results of flammability testing are listed in Table 5. As can be seen from the flammability testing results, also listed in Table 4, further incorporation of any of the tungstate in addition to MPP has very little effect on the burning properties of the composites especially with regard to the LOI values, where the presence of either AlW or SnW has no additional significant effect and the addition of ZnW showing a slight reduction and hence antagonism. However, there is a general minor improvement in the UL94 performance of all complex-containing samples in that at least two of the tested specimens for each sample achieved V-2 ratings and only one fails. It is interesting to note, however, that the pure PA66 sample had the same UL94 result

profile, which shows that the effects that any additive may have on reducing melt dripping (and so increasing the apparent flammability) may be equally offset by any accompanying flame retardant effect.

Table 5: Flammability parameters of MPP-containing formulations

Sample	UL94	LOI, vol%	Cone calorimetric data					
			T_{ig}, s	T_{fo}, s	T_{burn}, s	THR, s	PHRR, kW/m^2	R_{PHRR}, %
PA66	V-2/V-2/F	23.3	45	137	92	93	1544	-
MPP	V-2/F/F	27.3	41	174	133	93	715	53.7
AlW/ MPP	V-2/V-2/F	27.5	32	159	127	83	719	53.4
SnW/ MPP	V-2/V-2/F	27.3	33	159	126	90	653	57.7
ZnW/ MPP	V-2/V-2/F	26.2	35	166	131	103	604	60.9

Key: T_{ig}, T_{fo}, and T_{burn} are the times to ignition, flame out, total burn (= $T_{fo} - T_{ig}$) and peak heat release rate respectively (s), THR and PHRR are the respective total and peak heat release rates (kW/m^2). R_{PHRR}, % is the percentage reduction in PHRR with respect to PA66

Figure 3 shows the heat release curves for all samples in Table 5. It is evident that the presence of MPP significantly reduces the time-to-ignition, increases the time to flameout and reduces heat release rate and hence PHRR. The addition of each tungstate further reduces the time-to-ignition slightly with some further small reductions in PHRR values, apart from AlW and an increase in THR when ZnW is present. Apart from these slight difference, generally it would appear that addition of the three tungstates makes little overall difference to the burning properties of formulations containing MPP as the only flame retardant.

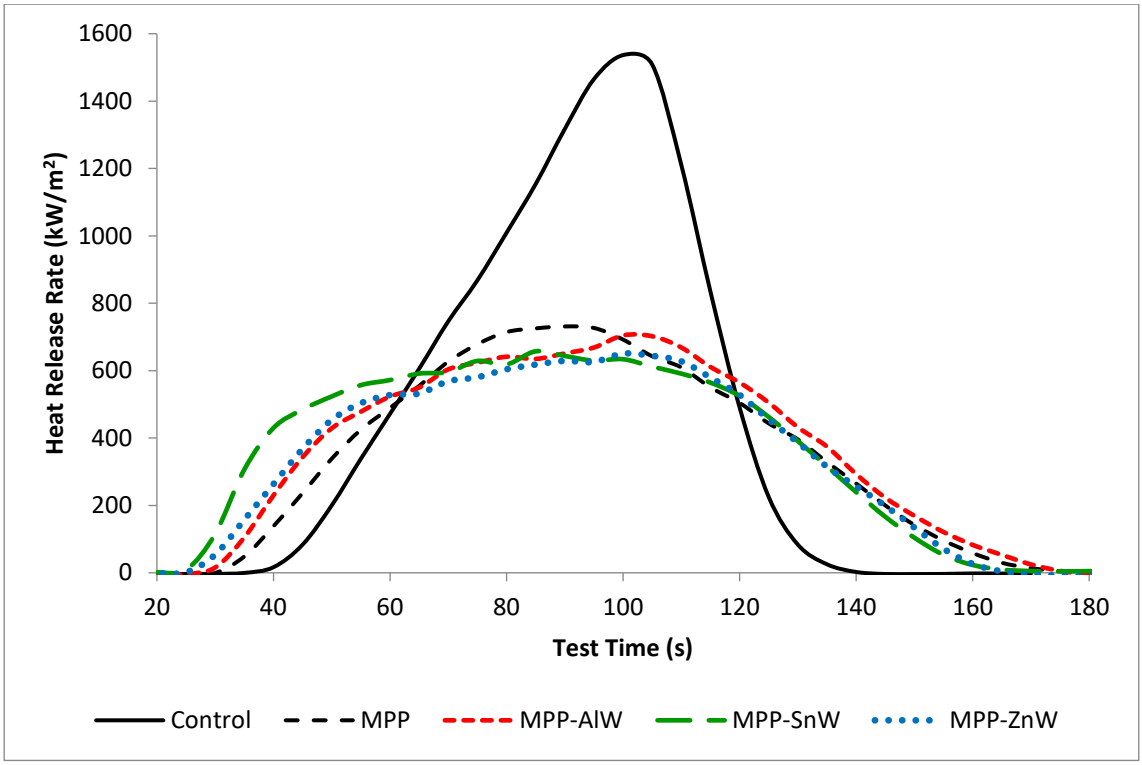

Figure 3: Heat release rate curves for PA66 samples containing MPP and each of the three tungstates.

3.3 TGA-FTIR Evolved Gas Analysis

The possible role of these tungstates on the flammability of PA66 will depend on the current understanding of its thermal degradation mechanism. While a number of significant studies of PA66 thermal degradation were undertaken over 60 years ago including the use of model compounds [18-21], this and subsequent research under an inert atmosphere, has been reviewed extensively by Schaffer et al [22] shows that PA66 thermal degradation is very complex and so only those reactions pertinent to this study will be discussed here. It is generally considered that PA66 thermally degrades by a primary random chain scission mechanism, whereby the polymer chains are broken through a pericyclic β-hydrogen elimination reaction, producing an amide and an alkene [22, 23] and also via scission of the C-N bond α to the amide carbonyl group [24] occurring in a random manner [25].

Through further reactions, and other more complex pathways related pathways, these products produce ammonia, cyclopentanone, and carbon dioxide [18 - 31].

In addition, PA66 is known to cross-link readily, especially under prolonged exposure to high temperatures,

where gelation is a notable occurrence [31, 32] and can make processing of PA66 problematic. It has been proposed that [31] condensation mechanisms driving the observed cross-linking of PA66 yield emissions of ammonia and secondary amines which react with primary amines to form cross-linking tertiary amines. Thus from these observations, emission of ammonia can be attributed as a prequisite for the cross-linking of PA66. Based on the above, the principal reactions relevant to this paper are summarised in Scheme 1.

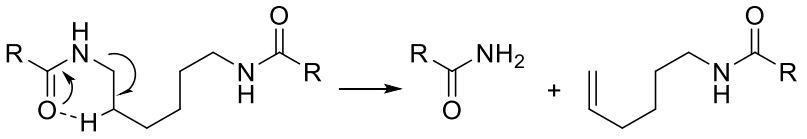

Main degradation reaction

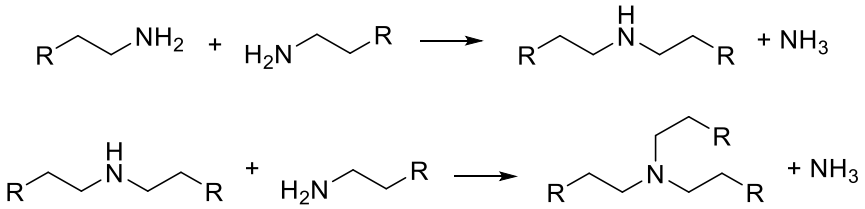

Elimination of ammonia from free amines indicative of cross-linking

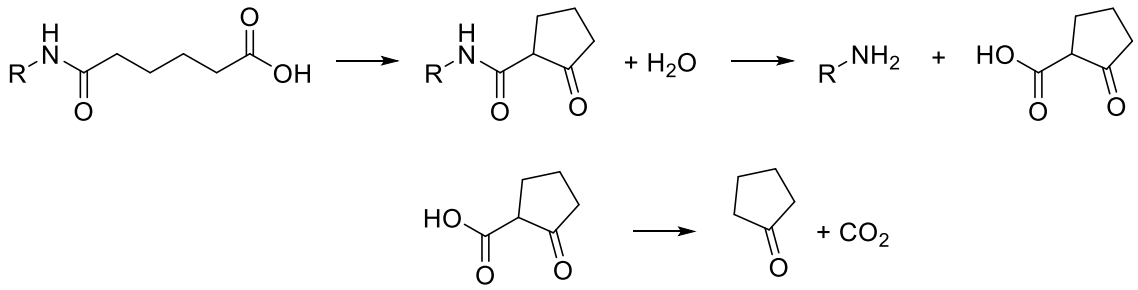

Formation of cyclopentanone and CO_2

Scheme 1: Principal thermal degradation routes of PA66 [18-31]

In the presence of oxygen, however, these mechanisms are modified, particularly at higher

temperatures, because of the lability of the hydrogen on the α-carbon atom adjacent to the amide nitrogen as is observed in both photo-oxidation [33] and wet oxidation [34]. Furthermore as stated previously [12, 17], the char residue increases several fold suggesting that oxygen-promoted cross-linking is occurring which might be a precursor to char formation in the presence of a suitable flame retardant [35].

Thus the key species produced during the thermal degradation of PA66 are carbon dioxide, an indicator of chain scission, cyclopentanone and other CH_x fuel species as primary flammable volatilse and ammonia, produced primarily by condensation reactions. These species were monitored during TGA using FTIR or mass spectrometry.

In order to identify CO_2 (at 2357 cm^{-1}), aliphatic fuel formers (including cyclopentanone) (at 2933 cm^{-1}, CH_x) and NH_3 (at 968 cm^{-1}), a set of specially compounded samples listed in supplementary Table T1 and having respective additive concentrations as listed in Table 3 were subjected to TGA-FTIR evolved gas analysis under both air and nitrogen. The formulations containing ZnW and either AlPi or AlPi/MPP were omitted because they showed the poorest flame retardant activity in Table 3. Exemplar FTIR spectra are shown in Figures 4(a), (b), (c) and (d) for the PA66 control and the PA66/AlW, PA66/AlPi and PA66/AlPi/AlW formulations respectively heated under air, where the time axes is a measure of TGA furnace temperature plus the 45s delay to allow for transfer of volatiles to the FTIR. It is observed that the majority of volatiles are recorded during the 20-25 minute period corresponding to the 400-600 ^oC region as indicated also in the respective TGA curves in Figure 1. In all spectra the peaks for CH_x (2933 cm^{-1}), CO_2 (2357 cm^{-1}) and NH_3 (968 cm^{-1}) are significantly evident with no signs of either the CO doublet at 2100 and 2200 cm^{-1}. The cyclopentanone C=O stretch absorption at 1750 cm^{-1} is also clearly evident, though some overlap with the NH_3 rotational bands between 1450 and 1800 cm^{-1} results in some interference, thus the C-H stretch was chosen for monitoring. Furthermore, no phosphorus oxy-acid absorptions were detected from samples containing AlPi and AlPi/MPP. These absences could be attributed to the short (c.a. 20 cm) path length of the FTIR cell and/or reaction with the heated metal gas line connecting the TGA output to the FTIR cell.

As stated in Section 2.4, the volumes of each gas produced were characterised by measuring the intensity of a specific peak over time. Exemplar gas/volatile evolution intensity versus temperature plots under

both air and nitrogen are shown in Figures 5(a) and 5(b) respectively, which were selected because the PA66/AlW/AlPi sample gave one of the highest R_{500} (23.3% in air) and LOI values (28.1 vol%) and consistent V-0 ratings, as well as a low R_{PHRR} value of 52.3%. A consistent feature of these traces, observed in all other samples as well, is that under air conditions, additional CO_2 shoulders or peaks arise in the 450-550 ^oC region and a further peak in the 550-650 ^oC region. These are a consequence of the oxidatively-formed char within the former region and its subsequent oxidation in the latter. The initial formation of CO_2 occurring over the 400-500 ^oC region coincides with the relative positions of the NH_3 and CH_x peaks. These peak intensities are little changed by the presence of air, which are indicators of char formation via deamination reactions [29] and fuel-forming reactions by chain scission reactions and formation of cyclopentanone and other flammable volatiles containing aliphatic C-H bonds. Thus the total area under the CO_2 emission vs temperature curves comprise three components, the first at 400-500 ^oC resulting from chain scission and related transitions, the second peak or shoulder at 450-550 ^oC from oxidative char formation [8] and the third above 550^oC to this char oxidation. It is possible that the third region has additional CO_2 from oxidation of CH_x products. The areas under the CO_2 emission vs temperature plots determined under nitrogen, which occur only in the 400-500 ^oC range, will reflect only the chain scission and related reactions and could be assumed to approximate to these same reactions even under air.

The areas under each of the respective gas/volatile evolution intensity versus temperature plots were recorded and then normalised to the respective PA66 control values under both nitrogen and air atmospheres and results are presented in Supplementary Table T1. The results are plotted in Figures 6(a) and (b) in order to assess the effects that AlW has on volatile formation and Figures 6(c) and (d) similarly with regard to SnW under both air and nitrogen atmospheres. The temperature corresponding to the time for this analysis can be calculated from the known heating rate and starting temperature of the TGA analyser (20 ^oC/min from 100 ^oC) and a set of temperature conversions is shown in Figure 4(d).

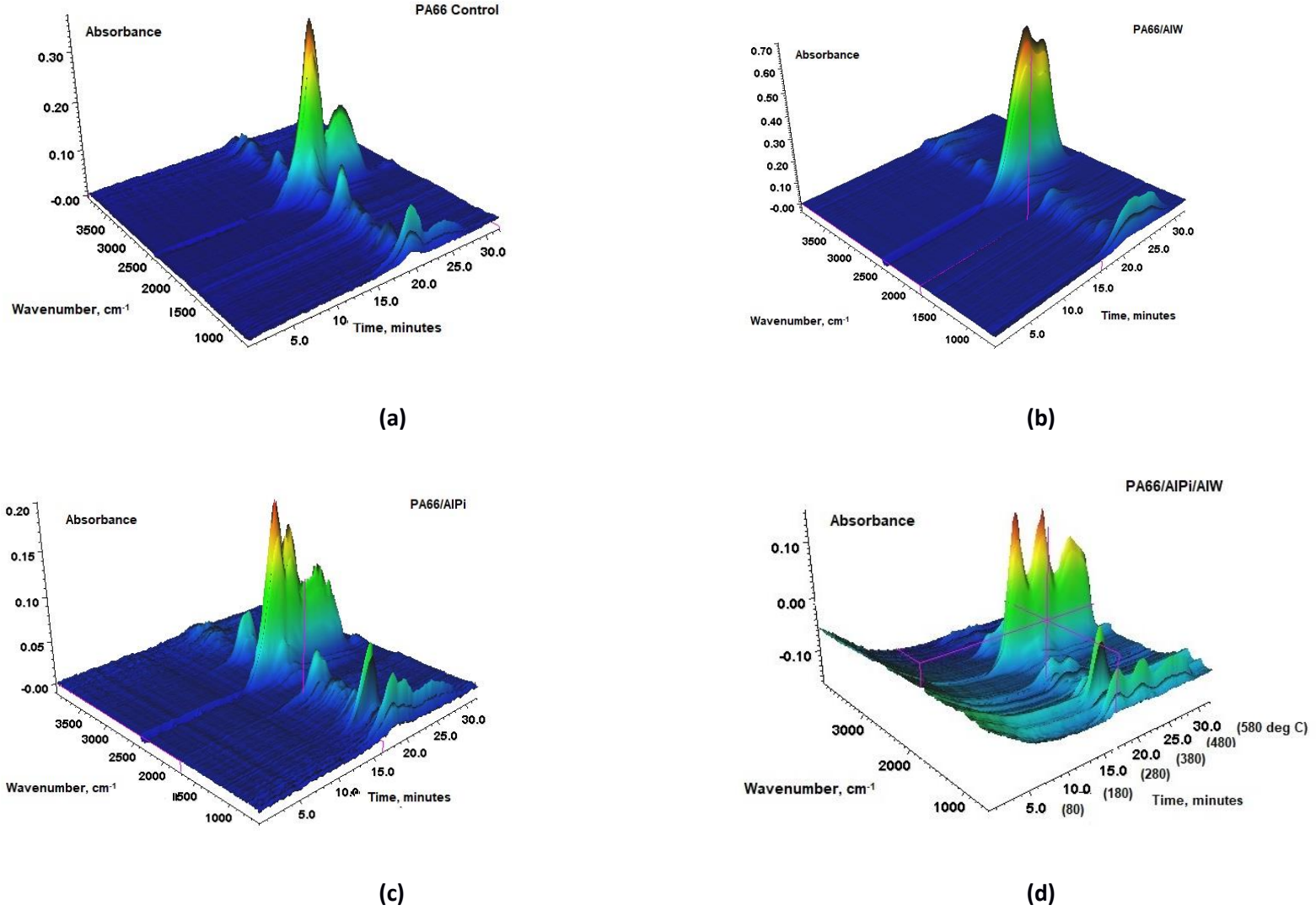

Figure 4: Exemplar TGA-FTIR curves under air conditions extracted at 450°C; (a) PA66 control, (b) PA66/AlW, (c) PA66/AlPi and (d) PA66/AlPi/AlW formulations (note the temperatures (°C) are inserted in brackets in (d).

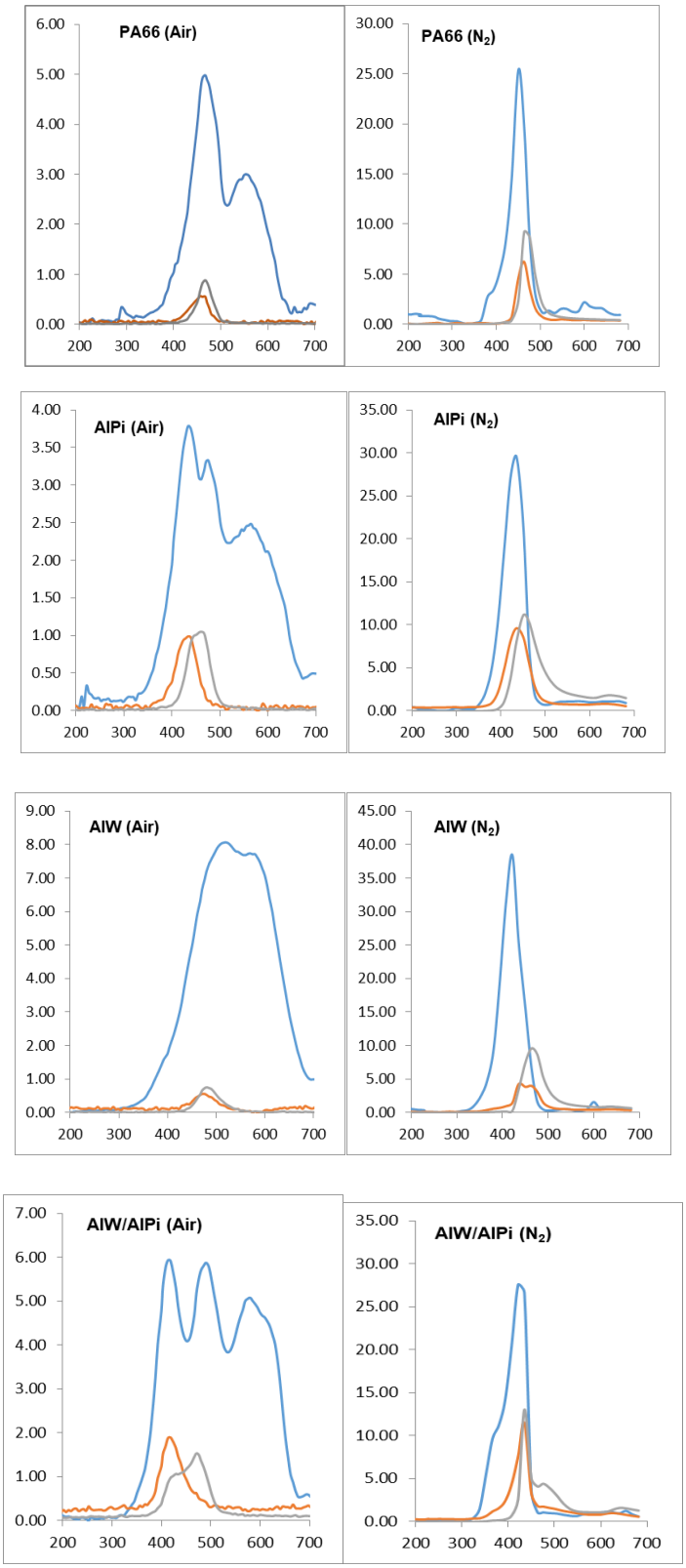

Figure 5: Exemplar gas/volatile evolution intensity versus temperature plots for PA66, PA66/AlPi, PA66/AlW and PA66/AlW/AlPi samples under (a) air and (b) nitrogen (Blue = CO_2; Orange = NH_3; Grey = CH_x); temperatures not corrected for ~45 s delay in FTIR with respect to TGA responses.

3.3.1 Effect of AlW and Phosphorus Flame Retardants

Figures 6(a) and (b) presents graphically the data listed in Supplementary Table T1 in order to assess the effects that aluminium tungstate in the presence and absence of either AlPi or AlPi/MPP has on the thermal degradation of PA66 under air and nitrogen respectively.

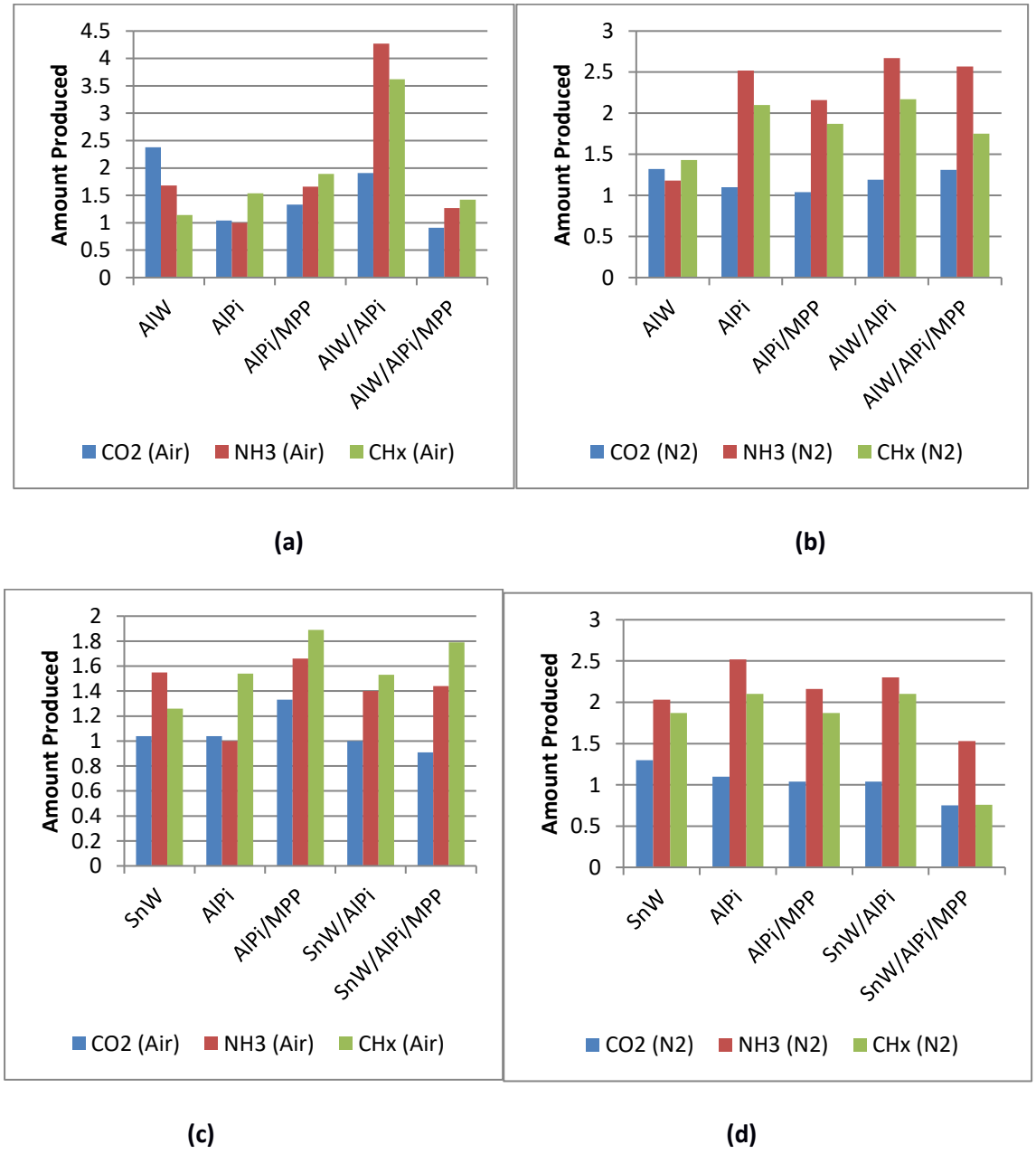

Figure 6: Relative amounts of CO_2, NH_3 and CH_x produced by (a) AlW in air, (b) AlW in nitrogen, (c) SnW in air and (d) SnW in nitrogen in PA6.6 composites containing either AlPi or AlPi/MPP (PA6.6 control =1)

Under nitrogen, AlW alone has little effect on the thermal degradation properties of PA66. The introduction of AlPi or AlPi/MPP alone, increases the formation of both ammonia and CH_x, in agreement with earlier work [22, 31, 32] and Scheme 1 in its promoting cross-linking and char formation in PA66. This effect is replicated when AlW is also present.

Under air, however, presence of AlW alone increases CO_2 production of PA66 significantly and NH_3 production moderately, while having a minimal effect on CH_x production. Again, the increase in NH_3 concentration is a possible indicator of increased cross-linking of the PA66 in agreement with the observed increase in char promotion and improved UL94 performance previously reported [12]. AlPi alone promotes only an increase in CH_x species while AlPi/MPP alone produces increases in all of the volatiles analysed with CO_2 production being least affected. The increased NH_3 production could be ascribed partly to the degradation of melamine [35]. Again, these changes suggest again an oxygen-influenced modification of the PA66 degradation pathways, with promotion of cross-linking and char as observed from TGA studies in Figure 1.

The PA66/AlW/AlPi composite volatile profile in Figure 6(a) is considerably different to that for PA66/AlPi under air although additional presence of AlW in the PA66/AlW/AlPi/MPP composite does not produce a similar effect when added to AlPi/MPP. These significant increases in NH_3 and CH_x species in the former are most likely linked to the superior fire performance of the AlW/AlPi formulation in PA66 reported in Table 3 in terms of its V-0 rating, high LOI (28.1 vol%) and high char formation (23.3 (18.3) wt%, see Table 2)). The AlW/AlPi/MPP formulation on the other hand shows similar char formation, has a low LOI value (25.5 vol%) and fails the UL94 test. Thus it would seem that enhanced char formation alone is not responsible for the superior fire performance of the AlW/AlPi formulation where major flame retardant activity is in the vapour-phase [15] whereas the added presence of MPP creates condensed phase, aluminophosphate formation [37]. However, the earlier work by Braun et al. [15] also indicated that addition of AlPi to PA66 increased CO_2 production accompanied by a reduction in CH_x production, which is in contrast to the for CO_2 and CH_x trends observed above. Clearly the role of added aluminium tungstate in increasing further the flame retarding effect of AlPi requires further investigation.

3.3.2 Effect of SnW and Phosphorus Flame Retardants

Figures 6(c) and (d) present the data in Supplementary Table T1 to show the effects that SnW in the presence and absence of either AlPi or AlPi/MPP has on the thermal degradation of PA66 under air and nitrogen respectively.

SnW increases NH_3 and CH_x production markedly under nitrogen indicating that the tungstate modifies PA6.6 thermal degradation suggesting that it enhances the char-promoting reactions as evidenced previously [12, 13] and this effect is little influenced by the presence of air. The effects of adding SnW to the AlPi formulation in PA66 are very similar to those observed when adding AlW in that the relative amounts of the three gases/volatiles measured are little changed in nitrogen (see Figure 6(d)) although in air (see Figure 6(c)) there is a relative decrease in NH_3. This possibly explains the slightly inferior UL94 fire performance relative to the AlW/AlPi formulation in Table 2, although LOI and char residue values are similar. While the volatiles profile in air for the SnW/AlPi/MPP composite is almost identical to that of the latter, its fire performance is much superior to that of its AlW-containing analogue (see Table 3) in terms of UL94 performance and higher R_{PHRR} value, although LOI and R_{500} values are similar. Again and like AlW, understanding how SnW influences the overall flame retardancy of AlPi and AlPi-containing PA6.6 composites is not simple, although some data correlations are seen to exist, including the high $Es_{(LOI)}$ values of>1 recorded for both SnW/AlPi and SnW/AlPi/MPP formulations.

3.4 Char analyses

In addition to the TGA-FTIR analysis carried out as described above, char analysis of retained cone calorimetric residues was also undertaken using FTIR and XRF to allow for determination of the organic and inorganic components present. The PA66 control tested by cone calorimetry left no residue at all and so could not be analysed.

3.4.1 FTIR Analysis

The char spectra are generally characterised by carbon-hydrogen absorptions of a largely aromatic char

structure and spectra for the AlW, SnW and ZnW control chars contain few intense peaks, with only weak shoulder absorbances at 1200 cm^{-1} (see Supplementary Figures S1 and S2). AlW in combination with AlPi or AlPi/MPP produces peaks corresponding to phenyl ring flexing, P=O peaks and alkyenyl hydrogens (C=C(-H)-C) at 1575, 1130 and 920 to 720 cm^{-1} respectively, suggesting the char is primarily aromatic in nature yet contains a degree of phosphoryl functionalities. A broad but weak depression at approximately 3400 cm^{-1} represents O-H functionalities either from hydroxyl groups or phosphorus acids. The alkenyl C-H groups (920 to 720 cm^{-1}), are more pronounced for the AlPi/MPP-containing sample. Similar observations can be drawn for the SnW and phosphorus-containing samples, which suggests that both AlW (with both P-containing flame retardants) and SnW (especially with AlPi/MPP) promote the formation of carbonaceous char in PA66.

3.4.2 XRF Analysis

Only AlW/AlPi/MPP and SnW/AlPi/MPP compositions were analysed as the AlPi-containing samples produced far less cohesive residues. XRF analysis are presented as ratios between the key elements, M:W:P where M = Sn or Zn, as elements lighter than Na are not readily detected. Al could not be accurately measured as the chars were supported on aluminium foil. These results enabled comparison with the theoretical ratios calculated from the starting composition of each sample to determine which elements had been retained in the char, and which were lost to the vapour phase (see Table 6).

Table 6: Summary of the absolute molar ratios between heavy elements in PA66 plaques and char samples normalised with respect to tungsten present in all samples (W = 1.000). Respective sample concentrations are those in Table 4.

Sample	P/W	W	Sn/Zn
AlW /AlPi/MPP plaque	3.617	1.000	-
Char	2.765	1.000	-
SnW/AlPi/MPP plaque	5.000	1.000	1.000
Char	2.928	1.000	0.911

The chars of AlW/AlPi/MPP and SnW/AlPi/MPP, while containing P=O species as indicated by FTIR, have lost a

proportion of their original phosphorus contents to the vapour phase relative to the amount of AlW or SnW retained. This would be expected as AlPi (66.7 wt% of AlPi/MPP), readily evolves diethylphosphinic acid [15]. The degree of phosphorus retained, however, could indicate that an amount of phosphorus from AlPi is retained in the condensed phase as respective metal phosphates including $AlPO_4$ [15, 37]. Any Al retention or loss from the AlW-containing sample could not be measured as outlined above, but the SnW-containing sample would appear to lose nearly 10 % of its Sn content, possibly to the vapour phase as SnO.

4. Discussion and Conclusions

The introduction of aluminium, zinc or tin (II) tungstates to PA66 not only has a char-promoting effect as evidenced previously [12, 13], but in the presence of selected phosphorus-containing flame retardant species can improve their flame retardant properties. It is most likely that the char-promoting character is based primarily on the Lewis acid catalysis of the condensation reactions, cross-linking and char-promoting mechanisms that are inherent during the thermal degradation of PA66 [22, 31, 32] and especially in the presence of oxygen [8, 16]. Each of the tungstates, may be considered to be the products of hypothetical reaction with the respective amphoteric oxides Al_2O_3, ZnO and SnO and tungsten trioxide, WO_3, which is weakly acidic with pH = 3.4-4.6 [38]. Based on an analysis of the relative behaviours of halides, the assessed Lewis acidic properties decrease in the order $AlX_3 > SnX_4 > ZnX_2$ [39]. However, in this work tin has the oxidation state of II and so the relative electron-attracting character of Sn^{2+} will be less than Sn^{4+}. Thus the previous Lewis acidity order may at best be summarised with regard to the three tungstates as AlW > SnW, ZnW. This order would explain why aluminium tungstate not only showed some evidence of flame retardant properties when present alone in PA66 [12], but also its superior activity when AlPi is also present, as shown by the high TGA residue in air at 500 ^oC (Table 2), LOI value and UL94 V-0 rating (Table 3). Results for the SnW/AlPi composite, however, are only slightly inferior in that V-ratings between V-2 and fail were noted. The ZnW/AlPi composite showed similarly poor UL94 performance and the lowest LOI and char at 500^oC values.

For AlW-containing composites, the added presence of melamine polyphosphate reduces the previous

level of flame retardancy, especially in now yielding a UL94 test "fail", probably because of formation of aluminophosphate species [17], which while retaining high TGA R_{500} and R_{580} residues in air (see Table 2) have contributed to the reduction in LOI to 25.4 vol% from a possibly, reduced Lewis acidic effect of AlW. In support of this hypothesis, the AlW/MPP formulation shows lower char formation at 500 ^{o}C than either the ZnW/MPP or SnW/MPP formulations (see Table 4). With regard to SnW/AlPi/MPP and ZnW/AlPi/MPP formulations, the addition of MPP has reduced the LOI of the latter and increased R_{PHRR} values (and hence $E_{s(PHRR)}$ values) of both composites relative to their MPP-free analogues.

TGA-FTIR studies further support an increased Lewis acid effect of AlW on the thermal degradation of PA66 in the presence of AlPi relative to the minimal effect when in the presence of AlPi/MPP where respective ammonia formations in air are in the ratio of about 4:1 although This difference in potential char-forming tendency is not reflected in their similar R_{500} and R_{580} values in Table 2. However, based on relative TGA-FTIR ammonia generating capacities, the SnW/AlPi composite generates about a third of the concentration of ammonia than the AlW/AlPi composite and generates lower R_{500} and R_{580} values, which possibly relates to the poor UL94 ratings (see Table 3) and lowest $E_{s(PHRR)}$ value (=0.55). However, that the SnW/AlPi composite has an LOI value >28 vol% and $E_{s(LOI)}$ > 1.0 suggests that the effect of SnW is one of suppression of the ignition stage rather than the post-ignition stage of combustion.

From this work, we can ascertain that in the system presented, additive rather than synergistic behaviour at best is observed. Finally it must be stressed that these reported results represent some initial studies into the behaviour of tungstates as potential flame retardants and while demonstrating promising results, it is recognised that significant further optimisation of formulations and investigations would be required before any possible commercial implementation were to take place.

5.0 Acknowledgements

We would like to thank the EPSRC and William Blythe Ltd for their support (CASE Studentship), and additionally Drs G. J. Milnes and G. Smart, Mr A. Zarei and Mr S. Shafiee for their technical support. We would additionally

like to thank William Blythe Ltd., and especially Mrs J. Redmayne, Mr D. Hilton, and Mr A. Ali for their assistance and access to analytical equipment.

5.0 References

1. Horrocks AR. Flame retardant and environmental issues, in: Update on flame retardant textiles: state of the art, environmental issues and innovative solutions. J. Alongi, A.R Horrocks, F. Carosio and G. Malucelli, editors, pp. 207–238, Smithers Rapra, Shawbury, UK, 2013.
2. Weil ED, Levchik, *Flame Retardants for Plastics and Textiles*. Munich: Carl Hanser Verlag, 2009
3. Papaspyrides CD, Kiliaris P, editors. *Polymer Green Fire Retardants*. Amsterdam: Elsevier BV, 2014.
4. de Wit C A, Herzke D, Vorkamp K. Brominated flame retardants in the Arctic environment — trends and new candidates. Sci Total Environ 2010; 408(15): 2885-2918.
5. Law RJ, Alaee M, Allchin C R, Boon J P, Lebeuf M, Lepom P, Stern G A. Levels and trends of polybrominated diphenylethers and other brominated flame retardants in wildlife. Environ Int 2003; 29(6): 757-770.
6. Cusack P, Hornsby P. Zinc stannate-coated fillers: novel flame retardants and smoke suppressants for polymeric materials. J Vinyl Addit Technol 1999: 5(1); 21-30.
7. Kicko-Walczak, E. Studies on the mechanisms of thermal decomposition of unsaturated polyester resins with reduced flammability. Polym Polym Comp 2004; 12: 127–134.
8. Horrocks AR, Smart G, Kandola BK, Holdsworth AF, Price D. Zinc stannate interactions with flame retardants in polyamides; Part 1: Synergies with organobromine-containing flame retardants in polyamides 6 (PA6) and 6.6 (PA6.6). Polym Degrad Stab 2012; 97(12): 2503-2510.
9. Horrocks AR, Smart G, Kandola BK, Price D. Zinc stannate interactions with flame retardants in polyamides; Part 2: Potential synergies with non-halogen-containing flame retardants in polyamide 6 (PA6). Polym Degrad Stab 2012; 94(4): 645-652.
10. Rothon R, Hornsby PR. Flame retardant fillers for polymers. In: Papaspyrides CD, Kiliaris P, editors. Polymer green fire retardants. Amsterdam: Elsevier BV, 2014. p. 289-322
11. Holdsworth AF, Horrocks AR, Kandola BK, Price D. The potential of metal oxalates as novel flame retardants and synergists for engineering polymers. Polym Degrad Stab 2014; 110: 290-297.
12. Holdsworth AF, Horrocks AR, Kandola BK. Synthesis and thermal analytical screening of metal complexes as potential novel fire retardants in polyamide 6.6. Polym Degrad Stab 2017; 144: 420-433
13. Holdsworth AF. Novel multifunctional fire and smoke retardants for engineering polymers, PhD Thesis, Bolton, 2014
14. Hörold S, Phosphorus-based and intumescent-based flame retardants. In: Papaspyrides CD, Kiliaris P, editors. Polymer green fire retardants. Amsterdam: Elsevier BV, 2014, pp.221-254

15. Braun Bahr H, Schartel B. Fire retardancy effect of aluminium phosphinate and melamine polyphosphate in glass fibre reinforced polyamide 6. E-polymers 2010; 94: 1–14
16. Lewin M, andEndo M. Intumescent systems for flame retarding polypropylene. In Fire and Polymers II, Nelson (editor), American Chemical Society Symposium Series 1995; 599: 91-117
17. Samyn F, Bourbigot S. Thermal decomposition of flame retarded formulations PA6/aluminum phosphinate/melamine polyphosphate/organomodified clay: Interactions between the constituents. Polym Degrad Stab 2012; 97: 2217-2230
18. Achhamme BG, F. W. Reinhart, Kline GM. J Res Natl Bur Std 1951; 46: 391
19. Hopff H. Kuntstoffe 1952; 42; 423
20. Goodman I. The thermal degradation of 66 nylon. J Polym Sci 1954; 13: 175-178
21. Goodman I. The thermal degradation of 66 nylon: Further studies on the pyrolysis of di-n-butyl adipamide. J Polym Sci 1955; 17: 587-590
22. Schaffer M A, Marchildon E K, McAuley K B, Cunningham M F. Thermal non-oxidative degradation of nylon 6,6. JMS Rev-Macromol Chem Phys 2000; C40: 233-272
23. Bailey W, Bird CN. Pyrolysis of esters. XIII. Pyrolysis of amides. J Org Chem 1958; 23: 996-1001
24. Straus S, Wall LA. Pyrolysis of polyamides. J Nat Res Bur Std 1958; 60: 39-45
25. Straus S, Wall LA. Influence of impurities on the pyrolysis of polyamide. J Nat Res Bur Std 1959; 63A: 269-273
26. Meacock G. Production of fibres from 6, 6-, 6, 10- and 6-polyamides. J Appl Chem 1954; 4: 172-177
27. Ballistreri A, Garozzo D, Giuffrida M, Montuado G, Mechanism of thermal decomposition of nylon 66. Macromolecules 1987; 20 (12): 2991–2997
28. Ballistreri A, Garozzo D, Giuffrida M, Impallomeni G, Montuado G. Primary thermal decomposition processes in aliphatic polyamides. Polym Degrad Stab 1988; 23: 25-41.
29. Wiloth F. Zur thermischen zersetzung von Nylon 6.6. III. Messungen zur thermolyse von nylon 6.6 und 6.10. Makromol Chem. 1971; 144: 283-307.
30. Shaffer MA, Marchildon EK, McAuley KB, Cunningham MF. Thermal kinetics of nylon 66: experimental study and comparison with model predictions. Macromol React Eng 2007; 1: 563–577
31. L. H. Peebles, M. W. Huffman. Thermal degradation of nylon 66. J Polym Sci A-1 1971; 9: 1807-1822
32. Yoshizawa Y, Saito H, Nukuda N. A direct observation of the crosslinking unit in thermally degraded polyamides. J Polym Sci B Polym Lett 1972; 10: 145-151
33. Vachon RN, Rebenfeld L, Taylor HS. Oxidative degradation of nylon 66 filaments. Text Res J 1968; 38 (7): 716-728
34. Goncalves ES, Poulsen L, Ogilby PR. Mechanism of the temperature-dependent degradation of polyamide 66 films exposed to water. Polym Degrad Stab 2007; 92: 1977-1985
35. Camino G, Costa L, di Cortemiglia L. Overview of fire retardant mechanisms. Polym Degrad Stab 1991;

33: 131-154

36. Costa L, Camino G. Thermal behaviour of melamine. J Therm Anal 1988; 34: 423-429
37. Braun U, Schartel B, Fichera MA, Jager C. Flame retardancy mechanisms of aluminium phosphinate in combination with melamine polyphosphate and zinc borate in glass-fibre reinforced polyamide 6,6. Polym Degrad Stab 2007; 92: 1528-1545.
38. Perrin DD, dissociation constants of inorganic acids and bases in aqueous solution, Butterworths, London, UK, 1969, p.209
39. Satchell DPN, Satchell RS. Quantitative aspects of the Lewis acidity of covalent metal halides and their organo derivatives. Chem Rev1969; 69(3): 251-278

Polymer Degrad Stab: doi.org/10.1016/j.polymdegradstab.2020.109220

Supplementary Data

Tables:

Table T1: Normalised TGA-FTIR gas/volatile absorption intensities collected under air and N_2, normalised to respective pure PA66 values.

Sample	CO_2 (Air)	CO_2 (N_2)	NH_3 (Air)	NH_3 (N_2)	CH_x (Air)	CH_x (N_2)
Control	1.00	1.00	1.00	1.00	1.00	1.00
AlW	2.38	1.32	1.68	1.18	1.14	1.43
ZnW	1.06	0.92	1.16	1.24	1.11	1.34
SnW	1.04	1.30	1.55	2.03	1.26	1.87
AlPi	1.04	1.10	1.00	2.52	1.54	2.10
AlPi/MPP	1.33	1.04	1.66	2.16	1.89	1.87
AlW/AlPi	1.91	1.19	4.27	2.67	3.62	2.17
AlW/AlPi/MPP	0.91	1.31	1.27	2.57	1.42	1.75
SnW/AlPi	1.00	1.04	1.40	2.30	1.53	2.10
SnW/AlPi/MPP	0.91	0.75	1.44	1.53	1.79	0.76

Figures:

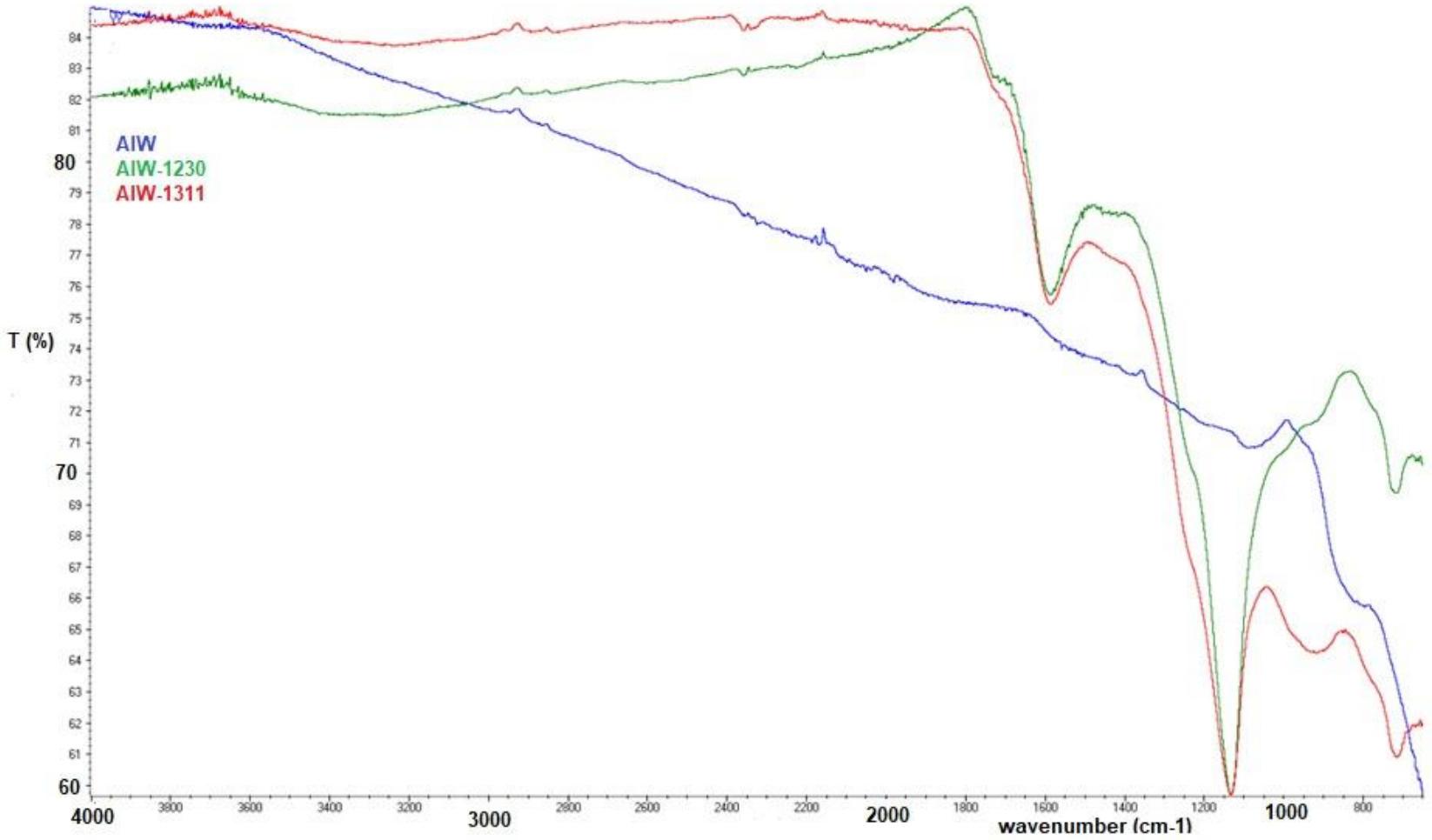

Figure S1: FTIR-ATR spectra, as percentage transmission, T%, of cone calorimetric chars PA66/AlW (blue), PA66/AlPi/AlW (green) and PA66/AlW/AlPi/MPP (red) composites

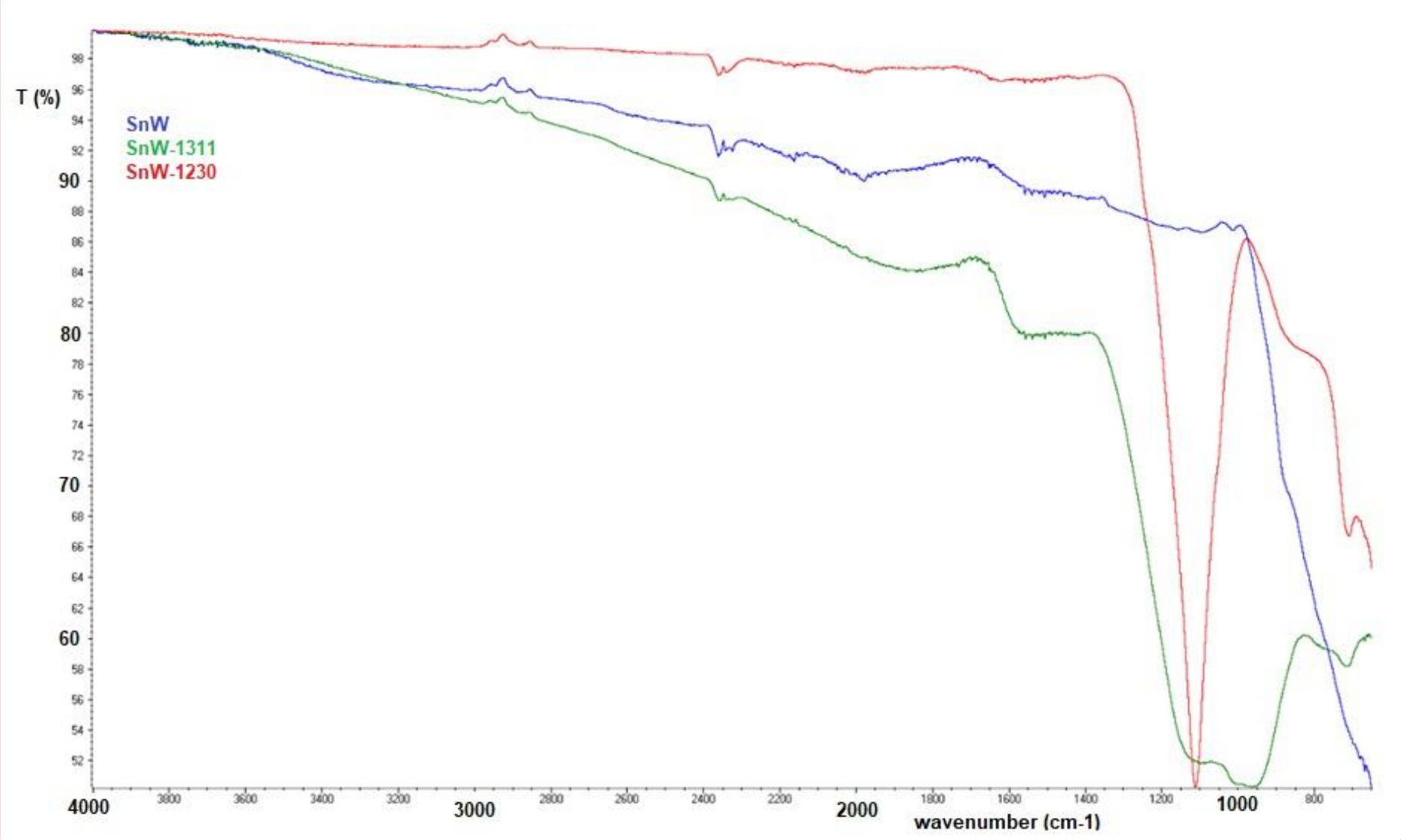

[GT1]

Figure S2: FTIR-ATR spectra, as percentage transmission, T %, of cone calorimetric chars of PA66/SnW (blue), PA66/SnW/AlPi (red) and SnW/AlPi/MPP

Polymer Degrad Stab: doi.org/10.1016/j.polymdegradstab.2020.109220

(green) composites.